An in situ CIR-FTIR investigation of process effects in the nickel catalyzed carbonylation of methanol

William R. Moser [a,*], Barbara J. Marshik-Guerts [a], Stanley J. Okrasinski [b]

[a] *Department of Chemical Engineering, Worcester Polytechnic Institute, Worcester, MA 01609, USA*
[b] *Eastman Chemical, Kingsport, TN 37662, USA*

Abstract

The carbonylation of methanol to form methyl acetate and acetic acid was investigated using phosphine modified nickel iodide as the metal catalyst precursor. The course of the reaction was monitored using a high pressure, high temperature in situ Cylindrical Internal Reflectance FTIR reactor (CIR-REACTOR) to acquire data under autogenous conditions. The capabilities of the reactor permit reaction monitoring at temperatures of 190°C and pressures of 13.6 kPa (1500 psig). In this study the reaction kinetics and in situ observations were made at temperatures between ambient and 160°C with an operating pressure of 8.16 kPa (900 psig) for most reactions. This study used methyl acetate as a solvent, and both methyl acetate and acetic acid were products of the catalytic reaction. Conditions were optimized at 160°C using organo-phosphine modified NiI_2 as the catalyst precursor. Under the applied reaction conditions, no anionic carbonyl species such as $Ni(CO)_x I_y^{-y}$ were detected at high carbonylation rates, in contrast to the anionic carbonyls reported in the rhodium catalyzed acetic acid process. In the rapid kinetic regime, only trace amounts of $Ni(CO)_4$ were formed in the reactor at steady state. The experimental results suggest a new mechanism involving $Ni(PPh_3)_2$ as one of the active metal complex intermediates reacting in a slow step with methyl iodide. The in situ reaction monitoring experiments readily enabled the determination of the concentrations of organonickel species as well as the concentration of carbonylation products under fast reaction conditions. © 1999 Elsevier Science B.V. All rights reserved.

1. Introduction

The rhodium catalyzed acetic acid process has been used extensively in industry for the production of acetic acid (AcOH) from methanol (MeOH). Due to the rising cost of rhodium, alternative metal catalysts such as Co, Ir and Ni have been investigated [1–4]. The earlier literature and patents on the Ni-based system indicated that severe process conditions were required for acetic acid formation from methanol [5–8]. The conditions included pressures as high as 26.7 kPa (200 atm) and temperatures in the range of 250–300°C in order to achieve significant production rates of acetic acid. Recently, the severity of the process conditions required for the Ni catalyzed acetic acid reaction was

---

* Corresponding author

decreased significantly by the use of organo-tin or organo-phosphorus promoters, thus, favorably competing with the Rh-catalyzed system [9].

Significant differences are seen in comparing the Ni-based system to the Rh-catalyzed process. For example, in the Ni catalyzed acetic acid process, the overall vapor pressure of solvent in the system must be lowered to achieve acceptable rates [10–14] in the intermediate pressure regime. Methanol is therefore diluted with a higher boiling co-solvent to obtain higher partial pressures of CO during the reaction [14]. A variety of co-solvents have been used including acetic acid, toluene, and methyl acetate. The corresponding acid for the carbonylation process is preferred for easier product separation.

It was found that the Ni species can be charged to the reactor in any form and need not be of very high purity [13,14]. This is also true for the reaction gases. Low grade CO has been used with impurities such as H_2O, N_2 and CO_2. It was reported [14] that the addition of H_2 significantly increases the reaction rate without producing any side products.

In order to obtain not only high reaction rates, but also high acetic acid selectivity, large quantities of an iodide promoter were added to the Ni catalyzed system [9,11]. The form of iodide added to the reaction was unimportant, but in general, methyl iodide (MeI) was used at a minimum mole ratio of 10:1, methanol to MeI [14]. High concentrations of iodide rapidly corrode the reactor; therefore, it was necessary to employ reaction conditions under which a high rate of reaction could be achieved while maintaining a low overall anionic $[I]$ concentration.

The reaction rates for the Ni-based system were significantly increased by the addition of a promoter such as an organo-phosphorus, -nitrogen, -tin, or -antimony complex [9]. The role of the promoter is still not understood. It is known that in the presence of MeI, both the organo-nitrogen and organo-phosphorus readily alkylate forming the corresponding quaternary salt [9]. No significant difference in the reaction rate was reported in prior studies between the various nitrogen and phosphorus complexes used as promoters, but in their absence no reaction occurred [2,3,9]. The motivation for this study is to provide fundamental information on the role of the promoter, effect of process parameters, and mechanistic evidence based on in situ reaction monitoring for the important intermediates in the active solutions. Such information is key in the design of a more efficient and cost effective catalytic system for an acetic acid process using no rhodium.

We report here the nickel catalyzed carbonylation of methanol to produce methyl acetate and acetic acid using an in situ Cylindrical Internal Reflectance Fourier Transform Infrared (CIR-FTIR) reactor (Fig. 1) which we have successfully applied in the past for the elucidation of several other mechanisms of homogeneous metal catalyzed chemical processes [15–22]. Our studies on this system employed the CIR-FTIR reactor operating under typical high temperature and high pressure reaction conditions simulating the high production rate conditions reported in the patent literature. Since the technique is truly an in situ method, providing real time analysis under autogenous conditions, it is useful for examining both process effects on the course of product formation as well as the identification and concentration determination of catalytic intermediates.

This study deals with process effects and the identification of catalytic nickel intermediates in the non-aqueous, methanol–methyl acetate, solvent system while a phosphine modified nickel catalyst converts methanol and CO to a mixture of methyl acetate and acetic acid. One objective of this study was to provide some direct observations from the in situ reactor studies concerning the slate of catalytically important nickel coordination complexes responsible for this conversion. We were particularly interested in identifying the reaction conditions which led to minimization of the $Ni(CO)_4$ concentration under steady state process conditions. The study also had the objective of determining the opti-
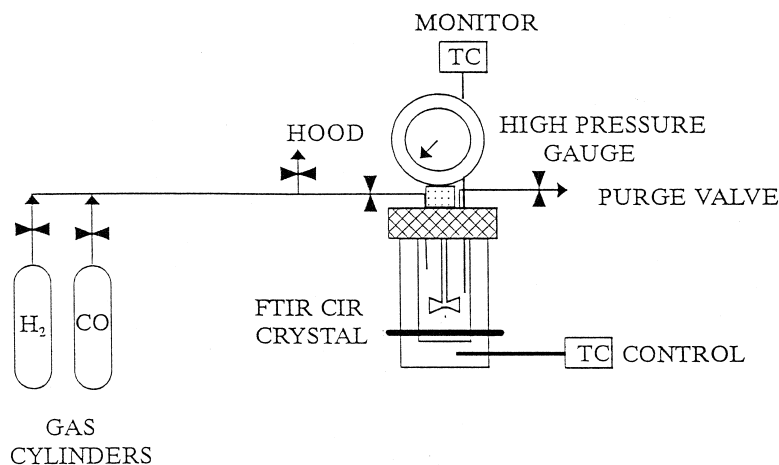
Fig. 1. Schematic of a high temperature and high pressure CIR-FTIR reactor [15] used in the infrared reaction monitoring experiments. The reactor is equipped with a silicon crystal mounted directly in the high pressure zone of the stirred autoclave.

mum reactant concentrations and reactor parameters for carrying out the detailed mechanistic study which will be reported in a subsequent paper. The final objective was to collect data for a comprehensive comparison between the reactions carried out here in a non-aqueous solution of methanol–methyl acetate to the more important mixed water–methanol solvent system. The subsequent paper reports the results from the methanol–water system as well as our detailed mechanistic conclusions and the role that phosphines play in promoting the reaction.

2. Experimental

The infrared spectra were collected using a Nicolet 510P FTIR located in a high velocity fume hood. An in situ CIR-FTIR reactor described previously [15] consisting of a stainless steel autoclave fitted with a monocrystalline silicon crystal is shown in Fig. 1. The autoclave top, purchased from PARR, was made of stainless steel and equipped with a high pressure gauge (18.1 kPa, 2000 psig), gas fill valves, and a direct drive mechanical impeller. For reactions using more corrosive, aqueous methanol sol-

vents, a CIR-REACTOR was used which was fabricated from all Hastalloy C parts.

The reactor was heated to 160°C over forty minutes during which time, 14 spectra of 50 scans per spectrum were taken in order to monitor the composition of nickel intermediates during heat-up. Higher temperatures, up to 190°C could be studied, but for the purposes of obtaining more accurate rate data, lower temperatures within the catalytic regime of 160°C, were used.

A co-solvent system of methanol and methyl acetate was used, in a 45:55 volume percent ratio, respectively. A standard reaction mixture contained a 0.2 M solution of NiI_2, a 0.75 M solution of LiI, a triphenylphosphine (PPh_3) promoter, methyl iodide (MeI), and both CO and H_2 gases. All the reactants, except the gases were added to the CIR-autoclave, fitted with Teflon seals, in a nitrogen flushed dry box. The autoclave reactor was then placed in the FTIR instrument and mounted in the CIR optical bench; then the reactor was purged three times with 2.72 kPa (300 psig) CO. CO at a pressure of 3.62 kPa (400 psig) was added followed by 0.91 kPa (100 psig) of H_2 gas to bring the total reactor pressure up to 4.53 kPa (500 psig) at room temperature. Spectra were taken after each step was completed in order to

monitor any changes that may have occurred during the addition of the various gases. After heating to a reaction temperature of 160°C, CO was again added to the autoclave bringing the final pressure to 8.15 kPa (900 psig). This pressure was maintained under operating conditions by continually charging CO into the reactor to replace CO consumed by reaction. Most of the experiments were run for three hours; at the end of which time most of the methanol was consumed. In all cases, the methanol carbonylation rates were calculated from the collected IR data during the steady state portion of the reaction profile, i.e., after about 10% methanol conversion.

After the experiment was terminated, the reactor was allowed to cool in the FTIR under a dry N_2 purge, to room temperature whereby additional spectra were taken. The pressure in the autoclave was then released slowly through a solution of isopropyl alcohol and I_2 in the hood to decompose any $Ni(CO)_4$ that may have formed during the reaction. The products were then analyzed by gas chromatography (GC) to check the infrared results.

Calibration curves for the extinction coefficient of methyl acetate and acetic acid were made at room temperature and at 160°C in a methanol solution. At the reaction temperature acetic acid and methanol esterified, forming methyl acetate and water in equilibrium amounts. It was therefore necessary to develop an alternative method for the determination of the extinction coefficient of acetic acid at process temperatures. A calibration curve was first obtained for acetic acid in methanol at room temperature by integrating the area under the peaks for acetic acid and plotting it vs. the known acetic acid concentration. A correction factor for the data at 160°C was then found by obtaining a spectrum of pure acetic acid at both room temperature and at 160°C in the reactor and determining the peak areas. The correction factor was then applied to all the room temperature calibration data, thereby obtaining a calibration curve for the concentration of acetic
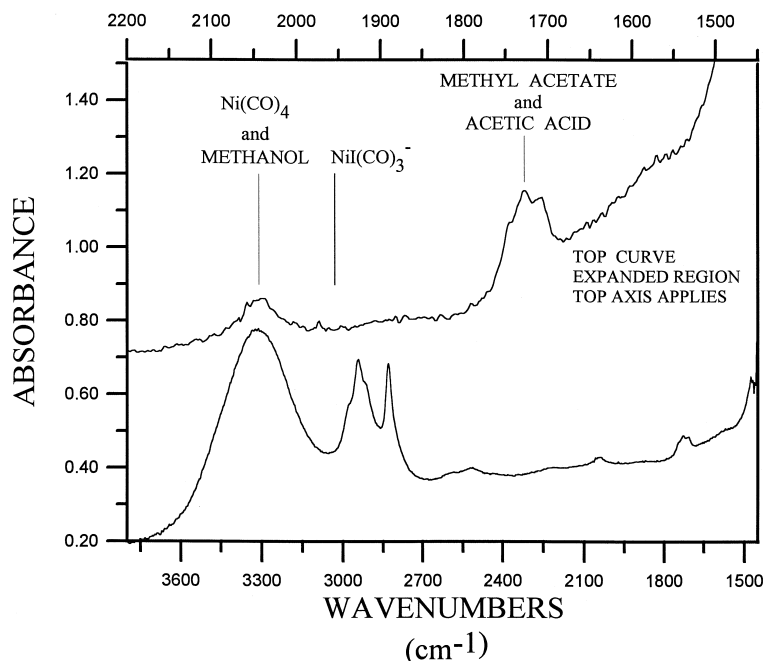

Fig. 2. Mid range infrared spectra of the Ni catalyzed carbonylation of methanol in a methanol–methyl acetate mixture under high rate conditions. The conditions used in this experiment were: a MeI/Ni mole ratio of 14.3; P/Ni—5.9; LiI—0.75 M, and 0.21 M NiI_2 in a 45% MeOH—55% MeOAc solution by volume at 160°C and pressurized with CO to 8.16 kPa (900 psig).

acid in methanol under reaction temperatures. Due to the severe overlap of the two product peaks, the reported carbonylation rate data includes both the areas of methyl acetate and acetic acid formed during reaction.

A series of experiments was run to establish a reasonable reaction rate from which a set of standard reaction conditions could be developed. The standard conditions were set at: (1) a MeI/Ni mole ratio of 14.3; (2) a P/Ni mole ratio of 2.9; (3) a 0.75 M solution of LiI; (4) a 0.21 M solution of NiI_2; and (5) a 45% MeOH and 55% MeOAc by volume mixture. Four series of reactions were performed by following the rate of methanol carbonylation as a function of: Ni concentration; MeI/Ni mole ratio, P/Ni mole ratio, and as a function of CO pressure.

The reaction was monitored by following a series of FTIR spectral peaks as a function of either time or temperature. Sample spectra showing various reaction and product components are displayed in Figs. 2 and 3. The spectral areas of interest include the acetyl region between 1850 cm^{-1} and 1650 cm^{-1}, the Ni carbonyl region between 2100 cm^{-1} and 1900 cm^{-1}, and the phosphonium region from 1620 cm^{-1} to 1460 cm^{-1}. Peaks of particular interest include $Ni(CO)_4$ (2044 cm^{-1}), $[Ni(CO)_3I]^-$ (1955 cm^{-1}), $MePPh_3^+I^-$ (1589 cm^{-1}), and PPh_3 (1585 cm^{-1}).

3. Results and discussion

Several series of carbonylation experiments were carried out using the triphenylphosphine–nickel iodide system to understand the relationship between reactant, promoter and catalyst concentrations, carbonylation rates and catalyst speciation. To illustrate the quality of spectra obtained using the CIR-REACTOR under typical nickel catalyzed carbonylation conditions, the mid-infrared region under conditions of high reaction rates is shown in Fig. 2. It is noted that the spectrum is void of any metal carbonyl absorption peaks with the exception of a trace amount of $Ni(CO)_4$. Before the reaction starts or when all of the methanol has been consumed, the $Ni(CO)_4$ concentration observable in the spectra are intense. These data are interpreted as evidence that the dominant form of the nickel catalyst at steady state, when acetic acid and methyl acetate are rapidly formed, contains no Ni–CO bond of any type. An important process consideration is that the concentration of $Ni(CO)_4$ may be kept to extremely low levels under steady state, high rate conditions. As will be shown later, the conditions required for optimum rates are the same as those required for $Ni(CO)_4$ minimization. Fig. 3, lower curve C, shows an expansion of the metal carbonyl region under conditions of optimum, rapid carbonylation conditions using a MeI/Ni ratio of 14.3. This spectrum illustrates the fact that neither $[Ni(CO)_3I]^-$ (1955 cm^{-1}), $Ni(CO)_4$, (2244 cm^{-1}) nor species of the type, $Ni(CO)(PR_3)_y$, were evident in solution under autogenous, facile product forming conditions. Curves A and B in Fig. 3, show that nickel carbonyls were ob-
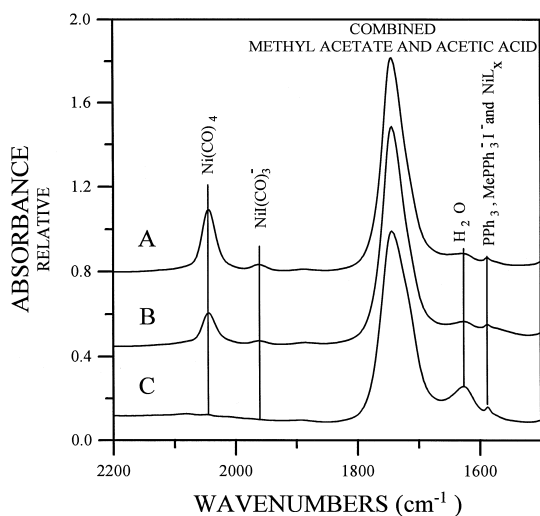

Fig. 3. Sample spectra showing the important metal carbonyl infrared bands and the typical signal to noise ratio for normal CIR-FTIR experiments as the MeI to Ni ratio is varied. (A) MeI/Ni ratio is 1.0, (B) MeI/Ni ratio is 2.8, (C) MeI/Ni ratio is 14.3. All reactions were at 160°C and pressurized with CO to 8.16 kPa (900 psig) and used P/Ni—3.0; LiI—0.75 M, and 0.21 M NiI_2 in a 45% MeOH—55% MeOAc solution.

Table 1

Run number	Rate	P/Ni	MeI/Ni	MeI/P
Constant MeI / Ni ratio				
1	0.0834	1.00	7.40	7.40
2	0.1151	3.10	7.36	2.37
3	0.1424	3.99	7.40	1.85
4	0.1775	5.06	7.43	1.47
5	0.0871	7.00	7.41	1.06
Constant MeI / P ratio				
Volume = 14 ml				
6	0.3506	3.17	4.59	1.47
7	0.2340	5.06	7.36	1.45
8	0.2343	7.02	10.30	1.47
9	0.2026	9.02	13.22	1.47
Volume = 21 ml				
10	0.1032	3.09	4.60	1.49
4	0.1775	5.06	7.43	1.47
11	0.1780	7.00	10.26	1.47
12	0.1408	8.98	13.16	1.47
Constant P / Ni ratio				
13	0.1872	3.09	14.34	4.64
14	0.1854	3.10	9.06	2.92
15	0.1677	3.10	8.18	2.64
2	0.1151	3.10	7.36	2.37
16	0.1071	3.09	5.99	1.93
17	0.1022	3.09	6.01	1.94
18	0.1017	3.10	4.60	1.48
10	0.1032	3.09	4.60	1.49
19	0.0470	3.10	3.00	0.97
Constant MeI$_{free}$ / Ni (5.08) ratio				
20	0.0961	2.00	7.08	3.54
15	0.1677	3.10	8.18	2.64
21	0.2694	4.00	9.07	2.27
22	0.2347	4.50	9.58	2.13
23	0.2249	6.00	11.78	1.96

served in solution under low rate conditions when low MeI/Ni ratios were employed.

The data on the observed carbonylation rates as a function of the various reaction parameters described below are compiled in summary form in Table 1. These relationships are discussed below as the total nickel concentration, CH_3I/Ni ratio, PR_3/Ni ratio, and total CO pressure were varied while monitoring carbonylation rates in real time by infrared.

3.1. Effect of nickel concentration

The effect of varying the Ni concentration on the methanol carbonylation reaction rate was examined under conditions where the P/Ni ratio was 2.9 and the MeI/Ni ratio was 14.3. The latter two ratios were held constant while the total Ni concentration was systematically varied. The results of these carbonylation reactions are plotted in Fig. 4. This figure shows that the reaction rates became steady after about 10% methanol conversion and were steady over a wide range of conversions. The region from 10% to 30% methanol conversion was also the regime of maximum rates for these reactions and was used in the kinetic evaluations. The maximum rates at steady state are plotted as a function of Ni concentration ([Ni]) in Fig. 5. The figure shows that the steady state carbonylation rate increased from a Ni concentration of 0.072 M to 0.120 M, whereupon the rate began to level off in the higher range of [Ni] of 0.145 M to 0.215 M. The effect of holding the MeI/Ni ratios constant has two effects on the reaction profile shown in Fig. 5, due to the fact that the total iodide concentration increased as the Ni concentration increased. As the Ni concentration increased in the low concentration range, the increasing iodide concentration contributed to the carbonylation rate increase, and as [Ni] increased in the high region, the effect of the large iodine concentration began to slow the
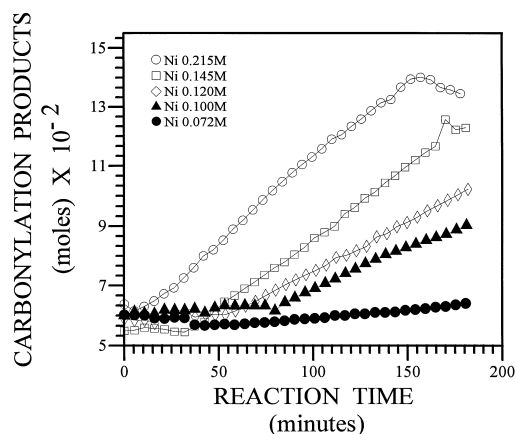

Fig. 4. Plot of the moles of carbonylated products formed vs. time as a function of Ni concentration at a reaction temperature of 160°C. The MeI/Ni ratio and P/Ni ratio were 14.2 and 2.9, respectively for all experiments.
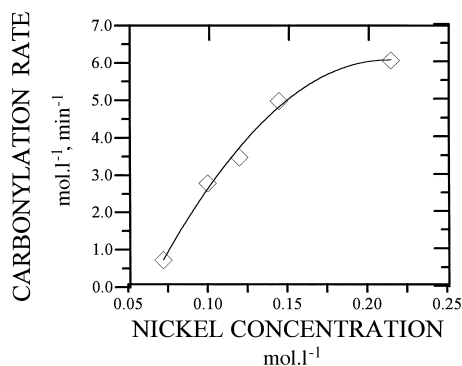
Fig. 5. Carbonylation reaction rate in moles of carbonylated products per liter per minute as a function of the Ni concentration in mole l^{-1}. Reaction conditions were the same as in Fig. 4.

Fig. 6. Plot of the variation of the $Ni(CO)_4$ peak area as a function of reaction time for five carbonylation experiments run as a functions of Ni concentration. The reaction conditions were the same as those in Fig. 4.

carbonylation rate. These data are consistent with the effect of increasing the iodide concentration on the carbonylation rate shown in a section below.

Fig. 6 illustrates a plot of the integrated infrared intensities of $Ni(CO)_4$ taken from low to high methanol conversions during the Ni concentration study. As the reaction proceeds, some trends appear in the $Ni(CO)_4$ data. At the highest nickel concentrations, where rates are highest, virtually no nickel carbonyl is formed in the reaction solution. Furthermore, all reactions showed $Ni(CO)_4$, at long reaction times after most of the methanol had been converted. Since the P/Ni ratio was 2.9 and the MeI/Ni ratio was 14.3, the total concentration of both the organophosphine and iodide are highest in the reactions where the Ni concentration is high. Thus, one would expect to observe lower $Ni(CO)_4$ concentrations due to bimolecular reactions between the phosphine or iodide and nickel species. The data in Fig. 6 also shows that the $Ni(CO)_4$ concentration is high during the induction periods (less than 60 min) where no carbonylation occurs, and it is significantly reduced in the high rate regime, with the exception of the lowest Ni concentration experiment. Fig. 7 is a graph of the steady state $Ni(CO)_4$ concentrations during the highest rate, steady state regime, and normalized to the original amount of Ni charged to the reactor. It is seen
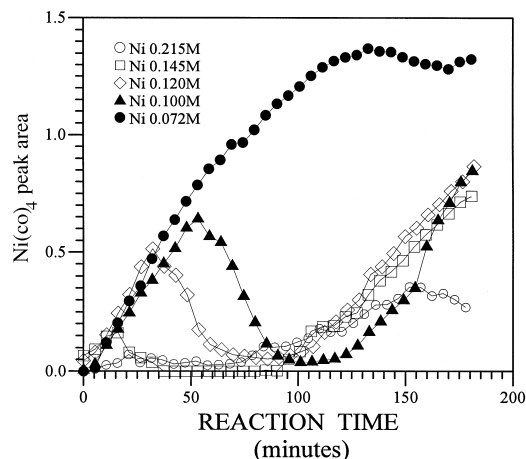
that at a [Ni] lower than 0.1 M, a significant amount of $Ni(CO)_4$ is produced; however, the Ni atom fraction in solution in the form of $Ni(CO)_4$ at concentrations greater than 0.10 M Ni is virtually zero. This data is important for understanding how to operate this type of process in the absence of $Ni(CO)_4$ formation.

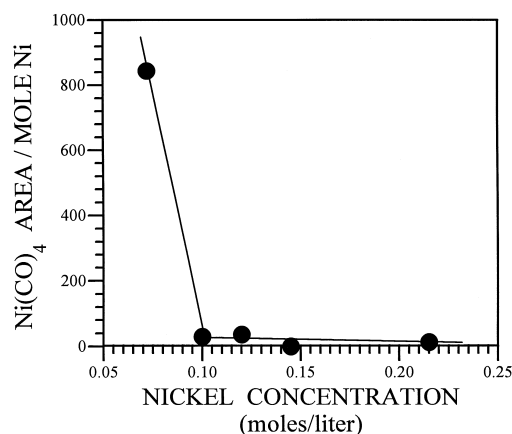Nelson [26] concluded that $Ni(CO)_4$ itself was not the active metal species, but that it may

Fig. 7. $Ni(CO)_4$ peak area normalized to the original amount of Ni in the reactor calculated at approximately 10% methanol conversion plotted vs. the Ni concentration. The reaction conditions were the same as those in Fig. 4.

be converted to the active form at higher [Ni] concentrations. Our data supports this conclusion in that Fig. 5 shows high rates and Fig. 7 shows very low $Ni(CO)_4$ concentrations at high nickel concentrations. Conversely, the rate of acetic acid and methyl acetate production decreases when high concentrations of $Ni(CO)_4$ appeared in the active solutions. This trend supports a competition between the formation of $Ni(CO)_4$ and the metal species within the active catalytic cycle. The appearance of $Ni(CO)_4$ in reactions using low Ni concentration likely resulted from the slow bimolecular rate of reaction between phosphine and $Ni(CO)_4$ due to the low concentration of both species. Alternatively, the equilibrium position of the $Ni(CO)_4$ reaction with phosphine would favor free nickel carbonyl under dilute conditions.

3.2. Effect of MeI / Ni ratio

In these experiments, the MeI concentration was varied while keeping the reaction conditions the same as described in Section 2 with a constant [Ni] of 0.21 M and a P/Ni ratio of 2.9. Thus, the ratio of MeI/Ni and MeI/P was altered while the results are reported as a function of the MeI/Ni ratio. Fig. 8 illustrates the carbonylation rates observed as the MeI/Ni ratio was altered. The figure shows that the rate
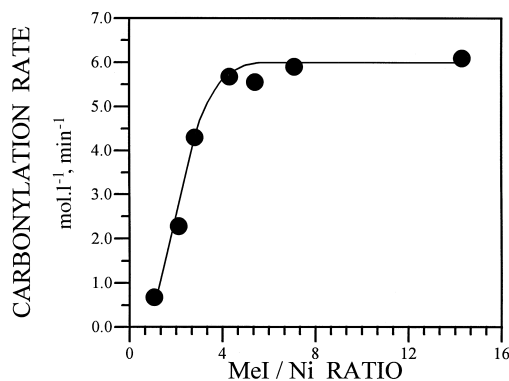

Fig. 8. Methanol carbonylation rate plotted as a function of the applied MeI/Ni ratio. Nickel concentration was maintained at 0.21 M; the P/Ni ratio was kept at 2.9, and the reaction temperature was 160°C.

increases as the MeI/Ni ratio increases up to a value of 4. It is seen that higher ratios have no effect on the rate. It was observed from Fig. 4 that nickel catalyzed carbonylations of this sort generally result in induction times which vary with reaction parameters. An examination of the kinetic plots (not shown here) for each of these reactions in the MeI/Ni variation series (Fig. 8) demonstrated that the induction time shortened as the MeI/Ni ratio increased. Similarly, an examination of the kinetics for the experiments used in Fig. 5 showed that the induction times were also shortened as the total Ni concentration increased.

The decrease in induction time as the Ni concentration increased is likely due to the fact that a catalytically active nickel–phosphine species forms more readily when both Ni and PR_3 concentrations are high. This conclusion is supported by the fact that the reactions involving long induction times (low Ni) demonstrated high concentrations of $Ni(CO)_4$ in their solutions at early times while those showing little or no induction time (high Ni) showed no $Ni(CO)_4$.

3.3. Effect of P / Ni ratio

The effect of changing the P/Ni ratio was also monitored by modifying the standard reaction parameters through a variation in the PR_3 concentration. Thus, the [Ni] was held constant at 0.21 M with a MeI/Ni ratio of 14.3 while the PPh_3 concentration was systematically altered. From the plot of methanol carbonylation rate vs. P/Ni ratio shown in Fig. 9, a maximum carbonylation rate occurred at a P/Ni ratio near 2, after which point the rate dropped as more PR_3 was added. Part of the rate decline was due to the fact that by keeping the MeI/Ni ratio constant, the amount of free MeI in solution decreased as the P/Ni ratio increased due to the reaction of PR_3 with MeI. Another series of experiments in which the P/Ni ratios were increased while the amount of free MeI in solution was held constant are shown in Table 1, experiments 20–23. These data show that the
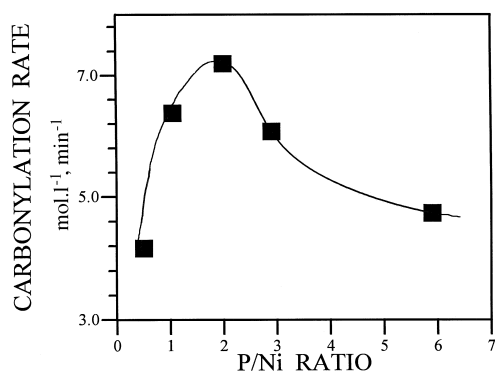
Fig. 9. Graph of the methanol carbonylation rate plotted as a function of the P/Ni ratio, keeping the Ni concentration constant at 0.21 M, the MeI/Ni ratio constant at 14.3, and the temperature at 160°C.

carbonylation rate also decreased as the P/Ni ratio increased, but the rate decline was not as sharp as when the MeI/Ni ratio was held constant as in Fig. 9. Thus, very high phosphine concentrations have a separate effect of slowing the carbonylation rate. One interpretation of this data is that as the PR_3 concentration increases, it reacts with the available Ni° species to form an equilibrium limited amount of an active species in the series of $Ni(PR_3)_n$ complexes. The addition of more PR_3 further reacts with $Ni(PR_3)_n$ to form $Ni(PR_3)_{n+1}$ which may be inactive toward methanol carbonylation. The evidence that the predominant catalytically active species in solution at steady state are $Ni(PR_3)_n$ type species rather than a Ni carbonyl complex is given by the fact that a careful examination of the in situ IR spectra for experiments used in the PR_3 variation study, shown in Figs. 9 and 10, demonstrated no nickel carbonyl species in the high rate, high PR_3 concentration regime. If $Ni(PR_3)_2$ were the most active of the $Ni(PR_3)_{4-n}$ complexes, it is reasonable that increasing the PR_3/Ni ratio from 0 to 6, as in Fig. 9, would lead to an initial increase in rate followed by a decline in rate. Due to the complexity of the large number of equilibrating species, we believe that the observation of a maximum rate near 2 as fortuitous. In reaction monitoring of catalytic systems by in situ tech-

niques, the observation of a discrete complex in solution as a predominant species at steady state can give rise to only two conclusion concerning its role relative to its participation within the principle catalytic cycle. It is either outside of the catalytic cycle and may serve as a reservoir to supply active metal to the catalytic cycle through equilibrating with one of the species in the cycle. The second possibility is that it is contained within the catalytic cycle and is specifically involved in the slow step in the active cycle. We suggest that the placement of $Ni(PR_3)_2$ within the catalytic cycle reacting with CH_3I in the slowest step in the active cycle is a reasonable possibility to rationalize our data. If this is the case, the results in Fig. 8 are expected due to the fact that the participation of CH_3I in a slow bimolecular reaction with $Ni(PR_3)_2$ would result in a linear increase in rate as the CH_3I concentration increases. However, the rate could level off if the expected bimolecular rate increase is offset by a decrease in the concentration of PR_3 by reaction with CH_3I. This reaction has the effect of decreasing the concentration of $Ni(PR_3)_2$ and CH_3I, both of which are reactants in the slow bimolecular rate controlling step. Although a combination of the in situ IR data and kinetic data suggest that $Ni(PR_3)_2$ is the active species in the catalytic cycle, this
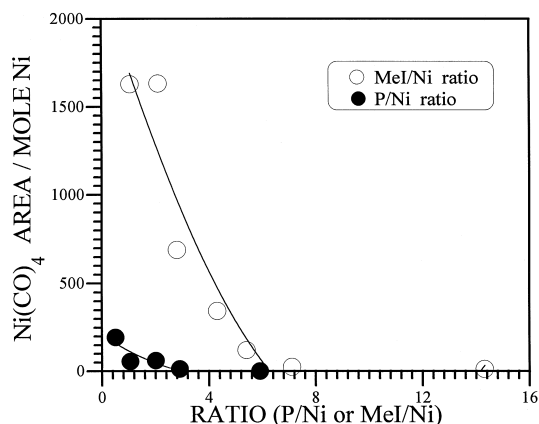
Fig. 10. Normalized $Ni(CO)_4$ peak area vs. the applied P/Ni ratio and against the MeI/Ni ratio. Reaction conditions were the same as those in Fig. 9.

IR technique does not have the resolution to distinguish between the various species of $Ni(PR_3)_n$.

A comparison was made in Fig. 10 of the normalized amount of $Ni(CO)_4$ formed in the steady state, high rate region for the two sets of experiments varying the P/Ni and the MeI/Ni ratios. It can be seen from Fig. 10 that by controlling the P/Ni ratio, the formation of $Ni(CO)_4$ was successfully suppressed over a wide range of P/Ni values. In the study where the MeI/Ni ratio was varied, a ratio of 7 was needed before any significant $Ni(CO)_4$ suppression was observed. However, as the P/Ni ratio was increased, the carbonylation rate increased, but significantly, the $Ni(CO)_4$ intensity decreased to trace amounts. This observation is important to setting the overall reactor parameters for operation with maximum carbonylation rates.

As noted above, Fig. 9 shows that a P/Ni ratio near 2 provided maximum carbonylation rates. If $Ni(PR_3)_2$ is the most active species in the $Ni(PR_3)_{4-n}$ series, one would expect to observe an increase in rate as $Ni(CO)_4$ is removed from solution to form the active species $Ni(PR_3)_2$. However, further additions of PR_3 would have the effect of removing the most active species to form $Ni(PR_3)_3$ or $Ni(PR_3)_4$ which are inactive.

3.4. Role of CO

The role of CO pressure upon the reaction rate was determined using a gas pressure switching experiment. The standard conditions were used: 2.9 P/Ni, 14.3 MeI/Ni and 0.21 M Ni concentration. The mixture was heated up to a reaction temperature of 160°C and then CO was added to bring the system pressure up to 8.16 kPa (900 psig). The reaction was allowed to run until the induction period was over and an active catalytic regime was established (approximately 40 min). The reaction was then allowed to drop in pressure to 7.25 kPa (800 psig) while the carbonylation rate was deter-

mined by IR. Once the next pressure was reached, it was maintained by adding CO and data were taken for forty minutes. This process was continued in stages until the reactor pressure reached 5.44 kPa (600 psig). The partial pressure of the solvent mixture at 160°C was subtracted from the total applied pressure to obtain the carbon monoxide partial pressure at each point. The kinetic analysis of this data resulted in the plot shown in Fig. 11, which illustrates that the CO dependence of the reaction rate is first order. The observation of a clean first order dependence on CO of the reaction rate indicates that if the bimolecular reaction between CH_3I and $Ni(PPh_3)_2$ is rate controlling, this step must be a rapid reversible equilibrium where the equilibrium position substantially favors reactants. CO is thought to react directly with a small equilibrium amount of the four coordinate addition product, from NiL_2 with CH_3I, to form a five coordinate acyl intermediate within the catalytic cycle which is transformed by subsequent fast steps to product. Since the in situ reaction monitoring of all of our experiments at steady state in the most active catalytic regime detected no metal acyl or carbonyls, this data is consistent with the above described partial mechanism.
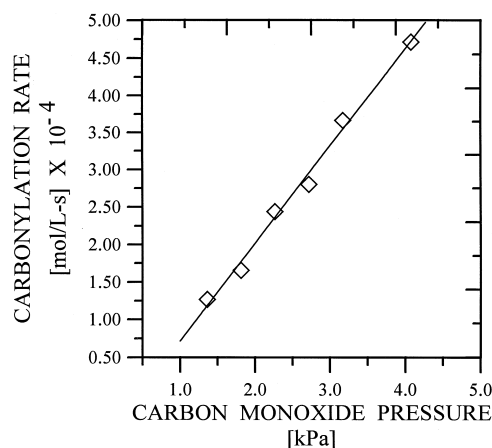

Fig. 11. Kinetic plot of first order dependence of CO pressure on the methanol carbonylation rate. The standard conditions applied were: 2.9 P/Ni; 14.3 MeI/Ni, 0.21 M Ni concentration, and a reaction temperature of 160°C.

3.5. Active metal species determination

Several experiments were performed to determine the variety of transient organonickel species formed during the initial period of heat up of the reactor to 160°C, within the induction period and within the high rate, steady state carbonylation period. During heat up of the reactions from ambient temperature to the reaction temperature, spectra were collected while recording both the corresponding temperature and pressure. Two or three Ni species were sometimes observed during the heat up process, of the form $[Ni(CO)_x(PPh_3)_y]$. In general the predominant species was $[Ni(CO)_3(PPh_3)]$ which was converted to $Ni(CO)_4$ once the temperature rose above 100°C. For the reactions that produced relatively high methanol carbonylation rates, all of the $[Ni(CO)_x(PPh_3)_y]$ species disappeared leaving only moderate concentrations of $Ni(CO)_4$ once the reaction temperature was reached. During the induction period the concentration of $Ni(CO)_4$ was further reduced. The fastest reactions using optimum amounts of phosphine and methyl iodide resulted in no carbonyl or acyl–metal complexes, and only trace amounts of $Ni(CO)_4$. Aside from solvent, reactant and product peaks, only IR bands due to $[P(CH_3)(PPh_3)_3]^+I^-$, PPh_3 and $Ni(PPh_3)_{4-n}$ were observed, and they were strongly overlapping. A typical steady state in situ spectrum taken under optimized conditions in the fast reaction rate regime is shown in Fig. 2 and the metal carbonyl and phosphine region is illustrated in Fig. 3.

At the reaction temperature of 160°C, but under non-optimum reaction conditions several in situ reactions monitored the concentrations of all species within the Ni carbonyl region of 2200 cm^{-1} to 1900 cm^{-1}. In this low rate regime, $[Ni(CO)_3I]^-$ appearing in the IR at 1955 cm^{-1} could be detected in low concentrations. No relationship at all was found between the intensity of the peak at 1959 cm^{-1} and increasing carbonylation reaction rates as the conditions were adjusted to approach the fast rate regime. Increasing the phosphine or methyl iodide concentrations reduced the amount of $[Ni(CO)_3I]^-$ to the point where it was not observable at the highest sensitivities of the instrument. These results are in disagreement with the general belief that $[Ni(CO)_3I]^-$ reported to absorb in the IR at 1955 cm^{-1} is one of the active metal species in the catalytic cycle [9,23–27]. In the case of the highest rate of reaction, where P/Ni = 2 and MeI/Ni = 14.3, the only infrared detectable Ni carbonyl species was trace amounts of $Ni(CO)_4$, and its concentration decreases in all experiments as the PPh_3 concentration increased. These results strongly suggest that neither $[Ni(CO)_3I]^-$ nor $Ni(CO)_4$ are intermediates in the active catalytic cycle.

An experiment was devised to starve the ongoing carbonylation reaction of CO while monitoring the species in situ. This procedure might slow the reaction down to the point where the CO addition step is rate limiting. Thus, it might then be possible to detect the organometallic species involved in the CO addition step, as was successfully done in a prior report [19,20] on palladium catalyzed carbonylations. The standard reaction conditions were used as described in Section 2 and run for approximately 50 min at 160°C. This ensured the reaction to be past the induction period and in the steady state, fast catalytic regime. After 50 min the CO supply was shut off and the temperature maintained at 160°C. Spectra were collected every two minutes, as the system pressure dropped due to CO consumption. The pressure profile was recorded along with the spectra until the CO consumption rate slowed to 0.045 kPa (5 psig) per 30 min. After the pressure dropped to 5.08 kPa (560 psig), the reaction was stopped. During the period of CO starvation, no new peaks in the region of 4200–1400 cm^{-1} were produced or consumed, other than acetic acid and methyl acetate production. The fact that the nickel speciation did not change during CO starving up to high CO pressure conditions, along with the observation of a first order CO rate dependence, is consistent with a catalytic

cycle involving the reversible reaction between $Ni(PPh_3)_2$ and CH_3I to form a four coordinate oxidative addition product in low concentrations in the equilibrium. If the oxidative addition reaction were not reversible, the CO starvation experiment would have resulted in build-up of the oxidative addition product, $[Ni(PPh_3)_2-(CH_3)(I)]$. This part of the mechanism is consistent with the fact that the oxidative addition reaction is normally reversible for most systems.

All of the elementary steps in the catalytic cycle after reaction with CO must be very fast since none of these intermediates could be observed in either fast or slow rate regimes. Also under no circumstance could acetyl iodide be observed. The details of the mechanism which have been indicated by this in situ process parameter study will be presented in a subsequent paper concerning the effects of ligands having varying electronic and steric structures. The mechanism of the nickel catalyzed conversion of methanol and CO to methyl acetate and acetic acid appears to be conceptually very similar to that which we proposed earlier for the palladium catalyzed carbonylation of bromobenzene, in methanol to produce methyl benzoate [19,20].

The mechanistic conclusions based on this study examining process effects while the slate of organometallic species were monitored by in situ infrared are summarized as follows. The data is consistent with $Ni(PPh_3)_2$ as an active species within the catalytic cycle, and is the dominant IR observable species appearing in the in situ experiments in low intensities between $1580–1590$ cm^{-1} overlapping with PPh_3 and $[MePPh_3]^+I^-$. The rate limiting step within the cycle is viewed as the reversible oxidative addition of MeI to $Ni(PPh_3)_2$ forming the four coordinate, $[NiI(CH_3)(PPh_3)_2]$ complex in low concentrations. The addition of CO to the oxidative addition product to form a transition state penta-coordinated $[NiI(CH_3)(CO)(PPh_3)_2]$ is viewed as fast. This type of species has been postulated before and similar penta-coordinated

Ni species are known to be moderately stable [27–29]. The reaction cycle rapidly continues with the $[NiI(COCH_3)(PPh_3)_2]$ species either reductively eliminating acetyl iodide with the regeneration of $Ni(PPh_3)_2$, or directly reacting with methanol to form methyl acetate. Since acetyl iodide was never detected in the experiments, even under high sensitivity in situ reaction monitoring, it is either immediately consumed by methanol or water forming acetic acid or methyl acetate; or the acetyl intermediate forms product by the direct reaction of methanol or water with $[NiI(COCH_3)(PPh_3)_2]$. Since the in situ infrared data shows the presence of $[MePPh_3]^+I^-$ in the reacting solutions from the very beginning to the end at high conversion, it is likely that this species reacts with the starting material, NiI_2, to form $[MePPh_3]_2[NiI_4]$. Indeed, this species may be formed in relatively high concentration and may tie up most of the Ni charged to the reactor. The function of hydrogen, which is essential for maintaining catalytic reactivity, may be to react with this complex forming $Ni°$ which rapidly reacts with unbound PPh_3 to replenish the active catalytic cycle with $Ni(PPh_3)_2$. The latter species is thought to be the dominant complex in solution under rapid carbonylation rate conditions. To show that the typical carbonylation solutions contained free PR_3 during catalysis, the amount of free PPh_3 was determined in a 0.55 M solution of $[MePPh_3]^+I$ in methanol at 160°C. This study showed that the phosphonium salt had dissociated to provide an equilibrium amount of 15% free PPh_3.

4. Conclusions

This study used kinetic and in situ infrared reaction monitoring to determine the observable organometallic species in the active solutions as the concentrations of reactants to the Ni catalyzed methanol carbonylation system were varied. In this way, a possible reaction mechanism, consistent with the experimental data was pro-

posed. The in situ reaction monitoring experiments showed that it is unlikely that either $[Ni(CO)_3I]^{1-}$ or $Ni(CO)_4$ are participants within the active catalytic cycle. These studies provided valuable process data on means to virtually eliminate the toxic material, $Ni(CO)_4$ from the reaction mixture. The effect of the combination of the data presented here in conjunction with a subsequent paper on the ligand effect on the carbonylation process enabled the construction of a detailed mechanism to be presented in the subsequent paper.

Acknowledgements

References

[1] D. Forster, T.C. Singleton, J. Mol. Catal. 17 (1982) 299.
[2] K. Fujimoto, K. Omata, T. Shikada, H. Tominaga, in: Yu. Yermakov, V. Likholobov (Eds.), Homogeneous and Heterogeneous Catalysis, VNU Science Press, Utrecht, The Netherlands, July 1986, p. 577.
[3] S. Matsuhira, Yuki Gosei Kagaku Kyokaishi 42 (1984) 115.
[4] M. Cheong, S.H. Lee, J.C. Kim, J.S. Lee, Y.G. Kim, J. Chem. Soc. Chem. Commun. 661 (1990) .
[5] W. Reppe, W. Schweckendick, Annalen 560 (1948) 104.
[6] W. Reppe, in: C.A. Meyer (Ed.) Acetylene Chemistry, 1949, p. 171.
[7] H. Adkins, R.W. Rosenthal, J. Am. Chem. Soc. 72 (1950) 4550.
[8] W. Reppe, H. Kroper, N. von Kutepow, H. Pistor, Justus Liebigs Ann. Chem. 582 (1953) 72.
[9] N. Rizkala, Am. Chem. Soc., Symp. Ser. 328 (1987) 61.
[10] E. Thomas, E. Alcook, U.S. Patent 2,650,245 (British Celanese), 1953.
[11] W. Reppe, H. Friederrich, N. von Kutepow, W. Morsch, U.S. Patent 2,729,651 (Badische Anilin- and Soda-Fabrik Aktiengesellschaft), 1956.
[12] W. Reppe, N. von Kutepow, H. Bille, U.S. Patent 3,014,962 (Badische Anilin- and Soda-Fabrik Aktiengesellschaft), 1961.
[13] A. Naglieri, N. Rizkalla, U.S. Patent 4,134,912 (Halcon International), 1979.
[14] A. Naglieri, N. Rizkalla, U.S. Patent 4,356,320 (Halcon SD Group), 1982.
[15] W.R. Moser, J.E. Cnossen, A.W. Wang, S.A. Krouse, J. Catal. 95 (1985) 21.
[16] W.R. Moser, C.C. Chiang, J.E. Cnossen, in: R.A. Condrate (Ed.), Adv. in Materials Character., Plenum, 1985, p. 315.
[17] W.R. Moser, J.E. Berard, R. Berger, P. Melling, Appl. Spectr. 46 (1992) 1105.
[18] W.R. Moser, ACS Adv. Chem. Ser. 230 (1992) 1.
[19] W.R. Moser, A.W. Wang, N.K. Kildahl, in: D.W. Blackburn (Ed.), Catal. Org. React., Dekker, New York, 1990, p. 137.
[20] W.R. Moser, A.W. Wang, N.K. Kildahl, J. Am. Chem. Soc. 110 (1988) 2816.
[21] W.R. Moser, C.J. Papile, D.A. Brannon, R.A. Duwell, S.J. Weininger, J. Mol. Catal. 41 (1987) 271.
[22] W.R. Moser, C.J. Papile, S.J. Weininger, J. Mol. Catal. 41 (1987) 293.
[23] T.W. Dekleva, D. Forster, Adv. Catal. 34 (1986) 81.
[24] J. Gauthier-Lafayre, R. Perron, in: Methanol and Carbonylation, Editions Technip (Paris, France), Rhône-Pulenc Recherches, Courbevoie, France, 1987, p. 117.
[25] S. Otsuka, A. Nakamura, Y. Yoshida, J. Am. Chem. Soc. 91 (1969) 7196.
[26] G.O. Nelson, Eastman Chemicals, Kingsport, TN, private communication.
[27] J.R. Zoeller, Eastman Chemicals, Kingsport, TN, private communication.
[28] C. Saint-Joly, A. Mari, A. Gleizes, M. Dartiguenave, Y. Dartiguenave, J. Galy, Inorg. Chem. 19 (1980) 2403.
[29] P. Stoppioni, P. Dapporto, L. Sacconi, Inorg. Chem. 17 (1978) 718.